Tunable Semiconductors: Control over Carrier States and Excitations in Layered Hybrid Organic-Inorganic Perovskites

Chi Liu,[1] William Huhn,[2] Ke-Zhao Du,[2] Alvaro Vazquez-Mayagoitia,[3] David Dirkes,[4] Wei You,[4] Yosuke Kanai,[4] David B. Mitzi,[2,1] and Volker Blum[2,1]

[1]*Department of Chemistry, Duke University, Durham, North Carolina 27708, USA*
[2]*Department of Mechanical Engineering and Materials Science, Duke University, Durham, North Carolina 27708, USA*
[3]*Argonne Leadership Computing Facility, 9700 South Cass Avenue, Lemont, Illinois 60439, USA*
[4]*Department of Chemistry, University of North Carolina, Chapel Hill, North Carolina 27599, USA*

(Received 19 March 2018; revised manuscript received 4 August 2018; published 4 October 2018)

For a class of 2D hybrid organic-inorganic perovskite semiconductors based on π-conjugated organic cations, we predict quantitatively how varying the organic and inorganic component allows control over the nature, energy, and localization of carrier states in a quantum-well-like fashion. Our first-principles predictions, based on large-scale hybrid density-functional theory with spin-orbit coupling, show that the interface between the organic and inorganic parts within a single hybrid can be modulated systematically, enabling us to select between different type-I and type-II energy level alignments. Energy levels, recombination properties, and transport behavior of electrons and holes thus become tunable by choosing specific organic functionalizations and juxtaposing them with suitable inorganic components.

DOI: 10.1103/PhysRevLett.121.146401

Hybrid organic-inorganic perovskites (HOIPs) [1,2], particularly three-dimensional (3D) HOIPs, are currently experiencing a strong revival in interest as economically processable, optically active semiconductor materials with excellent transport characteristics. Their success is showcased most prominently by record performance gains in proof-of-concept photovoltaic [3–12] and light-emitting devices [13–20]. The electronic function of 3D HOIPs can be tuned to a limited extent by manipulating the inorganic component (from which the frontier orbitals are derived), but the organic cations are confined by the 3D structure and are thus necessarily small (e.g., methylammonium [3–8,13–18] and formamidinium [9–11,19,21,22]), with electronic levels that do not contribute directly to the electronic functionality [23–28]. However, the accessible chemical space of HOIPs extends well beyond the 3D systems [1]. In particular, the layered, so-called two-dimensional (2D) perovskites do not place a strict length constraint on the organic cation. In these materials, a much broader range of functional organic molecules can be incorporated within the inorganic scaffolds, including complex functional molecules such as oligoacene or oligothiophene derivatives [1,29–37]. Fig. 1(a) shows the atomic structure of a paradigmatic example of such a 2D HOIP with active organic functionality, bis(aminoethyl)-quaterthiophene lead bromide AE4TPbBr$_4$ [34]. Similar juxtapositions of targeted organic and inorganic components give rise to a vast, yet systematically accessible, space of possible semiconductor materials [1,2,38–40], including those in which the molecular carrier levels contribute directly to the low-lying excitations and carrier levels [1,30–32,34,38,39,41]. This large space of conceivable organic-inorganic combinations thus offers the unique opportunity to tailor (ideally with computational guidance) materials with particularly desirable semiconductor properties, by intentionally controlling the spatial location and character of the electronic carriers and optical excitations throughout the material.

A key physical prerequisite to manipulate the semiconductor properties of layered hybrid materials is to understand the nature and spatial localization of their

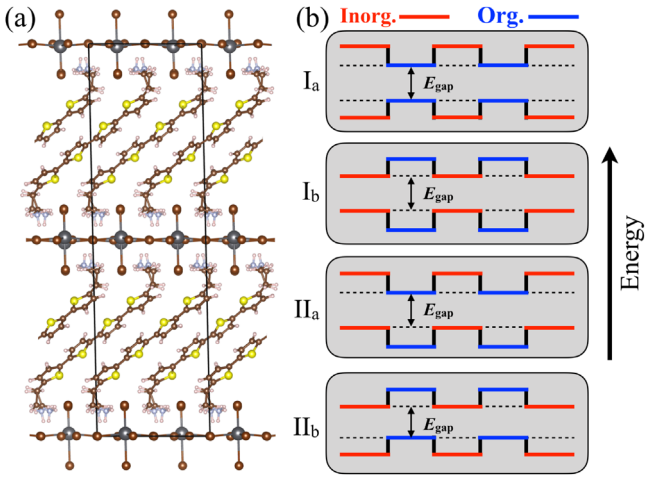

FIG. 1. (a) Structure of AE4TPbBr$_4$, fully relaxed by DFT-PBE + TS taking the experimental (x-ray diffraction) structure [34] as the input. (b) Possible energy level schemes (Ia, Ib, IIa, IIb) for the alternating organic-inorganic perovskite structure are shown, with the overall band gap indicated by arrows and dashed lines.

carriers and excitations. Specifically, the question of whether and exactly how one can understand their properties in analogy to quantum wells with varying confinement barriers (often assumed [40,42–44]) is subject to discussion in the literature [45–48]. Figure 1(b) exemplifies the principle by comparing four different conceivable quantum-well-like situations: "type I," with low-energy electrons and holes localized on the same component (either organic, Ia, or inorganic, Ib) or "type II," with electrons and holes on different components (holes on inorganic, electrons on organic, IIa, or vice versa, IIb). While some simple layered HOIPs have been successfully explained in a type-Ib picture (inorganic band edges with the organic acting as a quasi-inert screening medium [40,42–44,46–48]), a fully quantitative understanding of both band gaps within and band alignment between the materials' components is essential to recover the larger set of possibilities in Fig. 1(b). Providing this understanding for the large, complex crystal structures at hand constitutes a substantial challenge for current theory, both regarding computational resources and sufficiently accurate approximations. In this Letter, we demonstrate that these challenges can now be met, enabling us to answer questions that are central to future targeted developments of new HOIP semiconductors: (1) Can these structures be understood as quantum-well-like structures with spatially well-separated levels in the organic vs inorganic components, or will the electronic states be hybridized and thus delocalized across both components? (2) What is the spatial nature of electron and hole carriers within the structure? For instance, do they tend to migrate to the organic or the inorganic hybrid component in the lowest-energy configuration, drastically affecting each carrier's transport properties (bandlike inorganic vs hoppinglike organic)? (3) To what extent can we rationally tune the carrier and excitation properties by independently varying the organic and inorganic components?

Whether we can uncover a new paradigm using 2D HOIPs as "semiconductors on demand" with finely tunable properties and high-precision crystalline structural control depends on building a design principle that relates complex hybrid atomic structures to optoelectronic properties through answering the questions above. In this Letter, we do so through a first-principles theoretical examination of a class of oligothiophene-based 2D HOIPs, expanding on the $AE4TPbBr_4$ compound shown in Fig. 1(a). A practical challenge for theory is the structural complexity of these 2D HOIPs for which the unit cells are large. For instance, a (2×2) lateral supercell of the perovskite layer (Figs. S1–S3 in the Supplemental Material [49]) in this and other structures considered in this Letter is needed to cover the experimentally correct perovskite layer distortion and molecular arrangement, leading to 424 atoms in the simulation cell for $AE4TPbBr_4$. The (2×2) supercell instead of the experimentally reported (1×2) structure is necessary with regards to both accessing an energetically lower structure (Table S1 [49]) and also removing the disordering in the inorganic and organic structural components in the experimental structure. In addition, the two inorganic layers in the (1×2) relaxed structure have different Pb-Br-Pb angles, which disagrees with the experimental structure of $AE4TPbBr_4$ (Fig. S4 [49]). For structure predictions that capture the subtle balance of different molecular and inorganic bonding contributions, we use van der Waals corrected semilocal density-functional theory (DFT)—i.e., Perdew-Burke-Ernzerhof (PBE) exchange-correlation functional [55], plus the Tkatchenko-Scheffler (TS) pairwise dispersion scheme [56]. Electronic properties require a higher level of theory for qualitatively correct results, but the most attractive first-principles many-body approaches such as the *GW* approximation [57,58] remain out of reach for structures of this size. For band structure predictions, we therefore resort to the still demanding level of hybrid DFT using the Heyd-Scuseria-Ernzerhof (HSE06) functional [59,60], including spin-orbit coupling (SOC) [61]. Importantly, and unlike semilocal DFT, hybrid DFT in principle contains the right physics [62] to capture the frontier energy levels [valence band maximum (VBM) and conduction band minimum (CBM)]. Including SOC is critical to capture correctly the qualitative underlying nature of carriers, changing the nature of the CBM from "organic" to "inorganic" in $AE4TPbBr_4$ and reducing the band gap by ~0.3 eV (Fig. S5 [49]).

All calculations are performed by the FHI-AIMS code [57,61,63–68], using the ELSI infrastructure [67] and ELPA eigenvalue solver [69] for massively parallel simulations. For all crystal geometries, we employ full relaxation of unit cell parameters and cell-internal atomic coordinates [70], using the FHI-AIMS "tight" numerical defaults (Table S2 [49]) and k-point grid settings of $1 \times 2 \times 2$ (Table S3 [49]). For band structures, FHI-AIMS' "intermediate" settings (Table S4 [49]) and dense k-point grids of $3 \times 3 \times 3$ are used. The exchange mixing parameter in HSE06 was kept at 25% and the screening parameter at $\Omega = 0.11$ bohr^{-1} [71] in order to retain a single consistent base to compare energy band structures across different materials in this work. We first validate this approach for the low-temperature orthorhombic phase of $MAPbI_3$ [Fig. S6(a) [49]]. The lattice parameters predicted by DFT-PBE + TS agree with the experimental values [72] to within 1.4% [Fig. S6(b) [49]]. The HSE06 + SOC approach predicts a direct band gap of 1.42 eV, which underestimates the experimental value [1.65–1.68 eV, Fig. S6(b) [49]] by 0.2–0.3 eV [73,74]. Details of how we constructed the computational models for all structures considered in this Letter can be found in the Supplemental Material, Sec. IX [49]. For $AE4TPbBr_4$ [Fig. 1(a)], deviations of any unit cell parameters of the resulting predicted structure compared to experiment are 1.2% or better; i.e., they are in excellent agreement (Table S5 [49]). Finally, a new crystalline sample of $AE4TPbI_4$ was grown and an x-ray

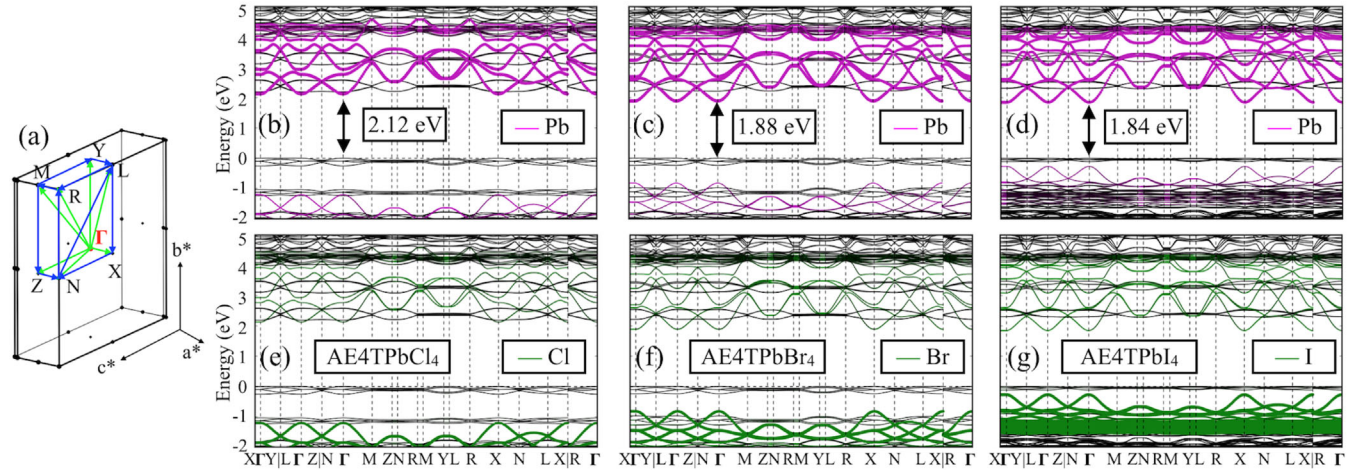

FIG. 2. Band structures of $AE4TPbX_4$ (X = Cl, Br, I) calculated by DFT-HSE06 + SOC with the states of Pb (b)–(d) and halogen (e)–(g) identified by projected density of states onto different species. The K path in the reciprocal space is shown in (a). The energy zero in (b)–(g) is set equal to the valence band maximum [for internal alignments relative to Pb 1s levels, see Fig. 3(a)].

structure refinement performed (Supplemental Material, Sec. X [49]), also indicating excellent agreement with the DFT-predicted structure used in the analyses below (Table S5 [49]).

Turning first to energy level localization, orbital plots (see Figs. S9–S11 [49] e.g., orbitals of $AE4TPbX_4$, X = Cl, Br, I) show that the states associated with inorganic and organic components are spatially well separated, supporting the notion of "quantum-well-like" states in these materials. This answers question (1) above and validates a discussion in terms of separate inorganic and organic bands. Even *et al.* [47,48] have also considered 2D HOIPs from the perspective of semiconductor quantum wells, showing that the effective mass model may fail due to the absence of superlattice coupling and importance of nonparabolicity. They proposed a computational analysis in terms of separate, neutralized organic and inorganic layers, appropriate for type-Ib situations. In the current Letter, we cover the full set of materials directly, allowing us to assess band gaps within each component as well as the alignments of their electronic levels. Knowing the alignments enables us to assess the full space of possible HOIP semiconductors (e.g., types I and II), where both the inorganic and the organic components are electronically active.

The halogen atoms in the inorganic framework offer a convenient handle for tailoring the associated electronic structure of the inorganic component by varying it from Br to Cl and I [34]. Full band structures for the compound series $AE4TPbX_4$ (X = Cl, Br, I) are shown in Fig. 2. All three compounds have a direct band gap at the Γ point. By changing the halogen, the dispersive bands originating from the inorganic component [Pb- and halogen-derived states, colored lines in Figs. 2(b)–2(g)] shift substantially with respect to the organic bands. In contrast, the organic-derived bands [black lines in Figs. 2(b)–2(g)] vary only slightly among these three compounds. Full and partial densities of states for these and other compounds in Figs. S14–S15 (Supplemental Material [49]) corroborate the chemical makeup shown in the band structures. Band curvature parameters (Table S6) that correspond to the diagonal elements of the effective mass tensors [75–77] in the reciprocal-space coordinate system of Fig. 2(a) confirm some qualitative trends emerging from the band structures: uniformly flat bands (effective masses $>20\ m_e$) perpendicular to the perovskite planes indicate hindered, nonbandlike transport. Somewhat lower effective mass tensor elements (2.2–11.4 m_e, still higher than in typical semiconductor materials) emerge for the holes (VBM) on the organic components parallel to the planes. Low effective mass tensor elements, $\approx$0.2–0.5 m_e, for the electrons (CBM) along the inorganic planes, in the range typical of 3D perovskites [76,77] might, absent other detrimental factors, indicate relatively easy electron transport.

The trends of the organic and inorganic frontier energy levels are shown in Fig. 3(a). The average of Pb 1s energy levels is chosen to formally align energy levels between different HOIPs in Fig. 3. However, we did not study how this choice (equivalent to the absence of dipolar fields between Pb ions across an interface between two different HOIPs) pertains to real interfaces between HOIPs, and the conclusions of this Letter do not rely on this convention. Replacing Br by Cl increases the overall computed band gap from 1.88 to 2.12 eV, whereas the substitution by I decreases the energy gap value to 1.84 eV. While the inorganic energy gap changes drastically from 2.70 to 3.32/2.11 eV for Cl/I substitutions (Fig. 3), the associated change in the organic energy gap is negligibly small ($\sim$0.1 eV). However, a drastic change evident from both Figs. 2 and 3(a) is the ordering of the levels, particularly the electronlike (CBM) states when going from Cl to Br and I.

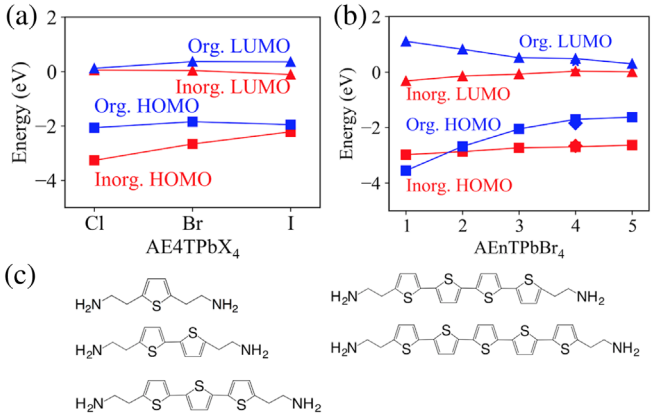

FIG. 3. (a) Frontier energy levels of the organic and inorganic components at the Γ point among the series of $AE4TPbX_4$ (X = Cl, Br, I). (b) Frontier energy levels at the Γ point among the series of $AEnTPbBr_4$ (n = 1–5). Stars and diamonds indicate the energy levels of syn-anti-syn $AE4TPbBr_4$ for $n = 4$. The average of Pb 1s energies is chosen to align the energy levels of different compounds. (c) Oligothiophene-based organic molecules considered in the all-anti configuration for varying the number n.

For Br and I, the band structures indicate type-IIb [Fig. 1(b)] quantum-well-like behavior; i.e., electrons and holes are expected to be spatially well separated on the inorganic and organic components, respectively. In contrast, the organic and inorganic CBM levels are predicted to lie within a few tens of meV for the Cl-substituted compounds; i.e., they are essentially degenerate within the uncertainties of the HSE06 + SOC treatment employed here. $AE4TPbCl_4$ is thus between types Ia and IIb in Fig. 1(b) and would allow electrons to travel to either component with reasonable ease at finite temperature. This difference would have profound implications for the expected carrier recombination properties of all three compounds, as evidenced, e.g., in photoluminescence (PL). In fact, strong quaterthiophene PL emission at ∼540 nm (2.30 eV) was experimentally observed for X = Cl [34], whereas the analogous PL features are substantially quenched for X = Br, I. Our present computational result agrees with and explains this experimental observation. While the X = Cl compound displays a near type-Ia band alignment, the X = Br, I compounds are clearly type IIb. In the latter two compounds, the energy level alignment therefore effectively impedes the electron-hole recombination since the electrons and the holes are preferentially located across the interface in the inorganic and organic hybrid components, respectively, i.e., addressing question (2) from the Introduction.

The importance of a fully predictive, quantitative theoretical treatment is further underscored by the fact that a discussion based on qualitative factors in 1999 led to the different conclusion of type-IIa, not type-IIb, alignment for this compound [34]. We note that optical excitations in absorption or emission cannot be expected to be captured based on the band structures derived in this work alone, since the typically strong excitonic effects are not included. For instance, exciton binding energies of up to 540 meV have been reported for 2D organic-inorganic perovskites [1,78] and an exciton binding energy of 0.4 eV has been reported in organic (not hybrid) sexithiophene thin films [79]. However, the qualitative localization of carriers prior to recombination (discussed above) still provides valuable insights into their expected recombination properties. We also note the potential implications of being able to tune levels on the organic and inorganic components independently, beyond optical properties, affects (e.g.) transport properties, dopability, and/or band offsets (and thus potential energy losses in devices) between the components.

We finally consider the ability to tune the band gap and quantum-well nature of the structure by varying the organic component, changing the conjugation length of the oligothiophene molecules. As shown in Fig. 3(b), we substitute the "all-anti" configuration (successive S atoms on alternating sides) of bis-ethylamine terminated oligothiophene AEnT [n = 1–5, Fig. 3(c)] into the scaffold of $AE4TPbBr_4$. While the quaterthiophene molecule in experimental $AE4TPbBr_4$ (Fig. 1) adopts a syn-anti-syn configuration [34], this configuration cannot be adopted by all AEnT (n = 1–5) oligothiophenes. For the purpose of having a systematic assessment, we thus restrict this part of our study to the all-anti configuration. Note, however, that the predicted electronic properties are only expected to be insignificantly affected by this conformational change as shown by the additional symbols corresponding to the syn-anti-syn conformation for $n = 4$ [Fig. 3(b)]. The electronic band structures reveal direct gaps for all considered conjugation lengths of $AEnTPbBr_4$ (Fig. S12 [49]) and band curvature trends (Table S7) are broadly consistent with those discussed for $AE4TPbX_4$ above. The overall band gap decreases as n increases, i.e., 2.66, 2.54, 1.98, 1.73, and 1.63 for n = 1–5, respectively. The predicted $AEnTPbBr_4$ compounds for n = 2–5 yield type-IIb level alignments. However, the $n = 1$ compound reveals a type-Ib alignment (both CBM and VBM derived from the inorganic component). This behavior (type Ib) is consistent with other 2D perovskites with smaller organic functionality, in which carriers or excitons are mainly funneled onto the inorganic subcomponent [46–48,80]. We thus affirmatively answer question (3) above—i.e., the carrier nature and neutral excitation properties and overall gap can be varied rationally by changing the organic component or the inorganic component in 2D HOIPs independently.

In summary, our results show that the quantum-well model can be used for conceptual understanding and as a useful starting point as a design principle for the layered HOIP family of hybrid materials. The tunability of electronic properties, exemplified by the materials studied in

this Letter, opens up the possibility to computationally predict and tailor nanoscale charge separation or recombination, as well as spatially separated charge transport within the much larger overall class of hybrid crystalline materials. Clearly, significant challenges would remain if theory were applied in isolation. For example, capturing all structural subtleties of complex 2D HOIP arrangements is nontrivial, as is predicting fundamental gaps with an accuracy of better than a few tenths of an eV (the accuracy expected from the unmodified HSE06 + SOC functional [71], as used in this Letter, for typical semiconductors [75,81,82]) for structures of this size. Excitingly, the combination of such predictions with subsequent targeted experimental syntheses overcomes these challenges, creating enormous possibilities to identify and fine-tune entirely new layered crystalline organic-inorganic semiconductors with deliberately selected optoelectronic or electronic properties.

This work was financially supported by the NSF under Awards No. DMR-1729297 and No. DMR-1728921, as well as through the Research Triangle MRSEC (DMR-11-21107). Computer time was provided by the Innovative and Novel Computational Impact on Theory and Experiment (INCITE) program and the Theta Early Science Program (ESP). This research used resources of the Argonne Leadership Computing Facility (ALCF), which is a DOE Office of Science User Facility supported under Contract No. DE-AC02-06CH11357.

[1] B. Saparov and D. B. Mitzi, Chem. Rev. **116**, 4558 (2016).
[2] W. Li, Z. Wang, F. Deschler, S. Gao, R. H. Friend, and A. K. Cheetham, Nat. Rev. Mater. **2**, 16099 (2017).
[3] A. Kojima, K. Teshima, Y. Shirai, and T. Miyasaka, J. Am. Chem. Soc. **131**, 6050 (2009).
[4] J. H. Heo, S. H. Im, J. H. Noh, T. N. Mandal, C.-S. Lim, J. A. Chang, Y. H. Lee, H. J. Kim, A. Sarkar, M. K. Nazeeruddin, M. Grätzel, and S. I. Seok, Nat. Photonics **7**, 486 (2013).
[5] D. Liu and T. L. Kelly, Nat. Photonics **8**, 133 (2014).
[6] N. J. Jeon, J. H. Noh, Y. C. Kim, W. S. Yang, S. Ryu, and S. I. Seok, Nat. Mater. **13**, 897 (2014).
[7] M. A. Green, A. Ho-Baillie, and H. J. Snaith, Nat. Photonics **8**, 506 (2014).
[8] P. Gao, M. Grätzel, and M. K. Nazeeruddin, Energy Environ. Sci. **7**, 2448 (2014).
[9] G. E. Eperon, S. D. Stranks, C. Menelaou, M. B. Johnston, L. M. Herz, and H. J. Snaith, Energy Environ. Sci. **7**, 982 (2014).
[10] W. S. Yang, J. H. Noh, N. J. Jeon, Y. C. Kim, S. Ryu, J. Seo, and S. I. Seok, Science **348**, 1234 (2015).
[11] W. S. Yang, B.-W. Park, E. H. Jung, N. J. Jeon, Y. C. Kim, D. U. Lee, S. S. Shin, J. Seo, E. K. Kim, J. H. Noh, and S. I. Seok, Science **356**, 1376 (2017).
[12] A. D. Jodlowski, C. Roldán-Carmona, G. Grancini, M. Salado, M. Ralaiarisoa, S. Ahmad, N. Koch, L. Camacho, G. de Miguel, and M. K. Nazeeruddin, Nat. Energy **2**, 972 (2017).
[13] Z.-K. Tan, R. S. Moghaddam, M. L. Lai, P. Docampo, R. Higler, F. Deschler, M. Price, A. Sadhanala, L. M. Pazos, D. Credgington, F. Hanusch, T. Bein, H. J. Snaith, and R. H. Friend, Nat. Nanotechnol. **9**, 687 (2014).
[14] J. Wang, N. Wang, Y. Jin, J. Si, Z.-K. Tan, H. Du, L. Cheng, X. Dai, S. Bai, H. He, Z. Ye, M. L. Lai, R. H. Friend, and W. Huang, Adv. Mater. **27**, 2311 (2015).
[15] Y.-H. Kim, H. Cho, J. H. Heo, T.-S. Kim, N. Myoung, C.-L. Lee, S. H. Im, and T.-W. Lee, Adv. Mater. **27**, 1248 (2015).
[16] H. Cho, S.-H. Jeong, M.-H. Park, Y.-H. Kim, C. Wolf, C.-L. Lee, J. H. Heo, A. Sadhanala, N. Myoung, S. Yoo, S. H. Im, R. H. Friend, and T.-W. Lee, Science **350**, 1222 (2015).
[17] Y.-H. Kim, H. Cho, and T.-W. Lee, Proc. Natl. Acad. Sci. U.S.A. **113**, 11694 (2016).
[18] Z. Xiao, R. A. Kerner, L. Zhao, N. L. Tran, K. M. Lee, T.-W. Koh, G. D. Scholes, and B. P. Rand, Nat. Photonics **11**, 108 (2017).
[19] X. Zhang, H. Liu, W. Wang, J. Zhang, B. Xu, K. L. Karen, Y. Zheng, S. Liu, S. Chen, K. Wang, and X. W. Sun, Adv. Mater. **29**, 1606405 (2017).
[20] S. Adjokatse, H.-H. Fang, and M. A. Loi, Mater. Today **20**, 413 (2017).
[21] D. B. Mitzi and K. Liang, J. Solid State Chem. **134**, 376 (1997).
[22] Q. Han, S.-H. Bae, P. Sun, Y.-T. Hsieh, Y. M. Yang, Y. S. Rim, H. Zhao, Q. Chen, W. Shi, G. Li, and Y. Yang, Adv. Mater. **28**, 2253 (2016).
[23] T. Umebayashi, K. Asai, T. Kondo, and A. Nakao, Phys. Rev. B **67**, 155405 (2003).
[24] F. Chiarella, A. Zappettini, F. Licci, I. Borriello, G. Cantele, D. Ninno, A. Cassinese, and R. Vaglio, Phys. Rev. B **77**, 045129 (2008).
[25] A. Filippetti and A. Mattoni, Phys. Rev. B **89**, 125203 (2014).
[26] F. Brivio, A. B. Walker, and A. Walsh, APL Mater. **1**, 042111 (2013).
[27] F. Brivio, K. T. Butler, A. Walsh, and M. van Schilfgaarde, Phys. Rev. B **89**, 155204 (2014).
[28] C. Motta, F. El-Mellouhi, S. Kais, N. Tabet, F. Alharbi, and S. Sanvito, Nat. Commun. **6**, 7026 (2015).
[29] M. Era, K. Maeda, and T. Tsutsui, Chem. Phys. Lett. **296**, 417 (1998).
[30] M. Braun, W. Tuffentsammer, H. Wachtel, and H. Wolf, Chem. Phys. Lett. **303**, 157 (1999).
[31] Z. Xu and D. B. Mitzi, Chem. Mater. **15**, 3632 (2003).
[32] K. Ema, M. Inomata, Y. Kato, H. Kunugita, and M. Era, Phys. Rev. Lett. **100**, 257401 (2008).
[33] K. Du, Q. Tu, X. Zhang, Q. Han, J. Liu, S. Zauscher, and D. B. Mitzi, Inorg. Chem. **56**, 9291 (2017).
[34] D. B. Mitzi, K. Chondroudis, and C. R. Kagan, Inorg. Chem. **38**, 6246 (1999).
[35] D. B. Mitzi, Inorg. Chem. **39**, 6107 (2000).
[36] X.-H. Zhu, N. Mercier, P. Frère, P. Blanchard, J. Roncali, M. Allain, C. Pasquier, and A. Riou, Inorg. Chem. **42**, 5330 (2003).
[37] M. Era, S. Yoneda, T. Sano, and M. Noto, Thin Solid Films **438–439**, 322 (2003).
[38] D. B. Mitzi, Prog. Inorg. Chem. **48**, 1 (1999).
[39] D. B. Mitzi, J. Chem. Soc. Dalton Trans. **2001**, 1 (2001).

[40] S. Zhang, G. Lanty, J.-S. Lauret, E. Deleporte, P. Audebert, and L. Galmiche, Acta Mater. **57**, 3301 (2009).

[41] D. Cortecchia, C. Soci, M. Cametti, A. Petrozza, and J. Mart-Rujas, ChemPlusChem **82**, 681 (2017).

[42] T. Ishihara, J. Takahashi, and T. Goto, Solid State Commun. **69**, 933 (1989).

[43] M. Era, S. Morimoto, T. Tsutsui, and S. Saito, Appl. Phys. Lett. **65**, 676 (1994).

[44] N. Wang *et al.*, Nat. Photonics **10**, 699 (2016).

[45] D. B. Mitzi, K. Chondroudis, and C. R. Kagan, IBM J. Res. Dev. **45**, 29 (2001).

[46] E. A. Muljarov, S. G. Tikhodeev, N. A. Gippius, and T. Ishihara, Phys. Rev. B **51**, 14370 (1995).

[47] J. Even, L. Pedesseau, and C. Katan, Chem. Phys. Chem. **15**, 3733 (2014).

[48] J. Even, L. Pedesseau, C. Katan, M. Kepenekian, J.-S. Lauret, D. Sapori, and E. Deleporte, J. Phys. Chem. C **119**, 10161 (2015).

[49] See Supplemental Material at http://link.aps.org/supplemental/10.1103/PhysRevLett.121.146401 for structural details of the perovskites in our simulations; energetic impact of the supercell choice; impact of spin-orbit coupling in the reported energy band structures; computational details (basis sets and k-space grid convergence); validation of computational protocols by comparing to experimental results for $MAPbI_3$, $AE4TPbBr_4$, and $AE4TPbI_4$; experimental details for the synthesis and characterization of a new $AE4TPbI_4$ crystal; and additional computed orbitals, energy band structures, band curvature parameters, full and partial densities of states supporting the general findings demonstrated in the actual work. Computational validation for $MAPbI_3$ also includes comparison to a more sophisticated many-body dispersion treatment [50]. Synthesis details include Refs. [51–53]. All computational input and output files (raw data) are available at the NOMAD repository [54].

[50] A. Ambrosetti, A. M. Reilly, R. A. DiStasio, Jr., and A. Tkatchenko, J. Chem. Phys. **140**, 18A508 (2014).

[51] H. Muguruma, T. Saito, A. Hiratsuka, I. Karube, and S. Hotta, Langmuir **12**, 5451 (1996).

[52] H. Muguruma, T. Saito, S. Sasaki, S. Hotta, and I. Karube, J. Heterocycl. Chem. **33**, 173 (1996).

[53] H. Muguruma, K. Kobiro, and S. Hotta, Chem. Mater. **10**, 1459 (1998).

[54] NOMAD Repository, https://doi.org/10.17172/NOMAD/2018.09.21-1 (accessed Sep 22, 2018).

[55] J. P. Perdew, K. Burke, and M. Ernzerhof, Phys. Rev. Lett. **77**, 3865 (1996).

[56] A. Tkatchenko and M. Scheffler, Phys. Rev. Lett. **102**, 073005 (2009).

[57] X. Ren, P. Rinke, V. Blum, J. Wieferink, A. Tkatchenko, A. Sanfilippo, K. Reuter, and M. Scheffler, New J. Phys. **14**, 053020 (2012).

[58] L. Reining, WIREs Comput. Mol. Sci. **8**, 1344e (2018).

[59] J. Heyd, G. E. Scuseria, and M. Ernzerhof, J. Chem. Phys. **118**, 8207 (2003).

[60] J. Heyd, G. E. Scuseria, and M. Ernzerhof, J. Chem. Phys. **124**, 219906 (2006).

[61] W. P. Huhn and V. Blum, Phys. Rev. Mater. **1**, 033803 (2017).

[62] J. P. Perdew, W. Yang, K. Burke, Z. Yang, E. K. U. Gross, M. Scheffler, G. E. Scuseria, T. M. Henderson, I. Y. Zhang, A. Ruzsinszky, H. Peng, J. Sun, E. Trushin, and A. Görling, Proc. Natl. Acad. Sci. U.S.A. **114**, 2801 (2017).

[63] V. Blum, R. Gehrke, F. Hanke, P. Havu, V. Havu, X. Ren, K. Reuter, and M. Scheffler, Comput. Phys. Commun. **180**, 2175 (2009).

[64] V. Havu, V. Blum, P. Havu, and M. Scheffler, J. Comput. Phys. **228**, 8367 (2009).

[65] S. V. Levchenko, X. Ren, J. Wieferink, R. Johanni, P. Rinke, V. Blum, and M. Scheffler, Comput. Phys. Commun. **192**, 60 (2015).

[66] I. Y. Zhang, X. Ren, P. Rinke, V. Blum, and M. Scheffler, New J. Phys. **15**, 123033 (2013).

[67] V. W. Yu, F. Corsetti, A. Garca, W. P. Huhn, M. Jacquelin, W. Jia, B. Lange, L. Lin, J. Lu, W. Mi, A. Seifitokaldani, A. Vazquez-Mayagoitia, C. Yang, H. Yang, and V. Blum, Comput. Phys. Commun. **222**, 267 (2018).

[68] A. C. Ihrig, J. Wieferink, I. Y. Zhang, M. Ropo, X. Ren, P. Rinke, M. Scheffler, and V. Blum, New J. Phys. **17**, 093020 (2015).

[69] A. Marek, V. Blum, R. Johanni, V. Havu, B. Lang, T. Auckenthaler, A. Heinecke, H.-J. Bungartz, and H. Lederer, J. Phys. Condens. Matter **26**, 213201 (2014).

[70] F. Knuth, C. Carbogno, V. Atalla, V. Blum, and M. Scheffler, Comput. Phys. Commun. **190**, 33 (2015).

[71] A. V. Krukau, O. A. Vydrov, A. F. Izmaylov, and G. E. Scuseria, J. Chem. Phys. **125**, 224106 (2006).

[72] M. T. Weller, O. J. Weber, P. F. Henry, A. M. Di Pumpo, and T. C. Hansen, Chem. Commun. (Cambridge) **51**, 4180 (2015).

[73] W. Kong, Z. Ye, Z. Qi, B. Zhang, M. Wang, A. Rahimi-Iman, and H. Wu, Phys. Chem. Chem. Phys. **17**, 16405 (2015).

[74] L. Q. Phuong, Y. Yamada, M. Nagai, N. Maruyama, A. Wakamiya, and Y. Kanemitsu, J. Phys. Chem. Lett. **7**, 2316 (2016).

[75] T. Zhu, W. P. Huhn, G. C. Wessler, D. Shin, B. Saparov, D. B. Mitzi, and V. Blum, Chem. Mater. **29**, 7868 (2017).

[76] N. Ashari-Astani, S. Meloni, A. H. Salavati, G. Palermo, M. Grätzel, and U. Roethlisberger, J. Phys. Chem. C **121**, 23886 (2017).

[77] J. Feng and B. Xiao, J. Phys. Chem. Lett. **5**, 1278 (2014).

[78] D. B. Straus and C. R. Kagan, J. Phys. Chem. Lett. **9**, 1434 (2018).

[79] I. Hill, A. Kahn, Z. Soos, and R. Pascal, Jr., Chem. Phys. Lett. **327**, 181 (2000).

[80] J. Even, L. Pedesseau, J.-M. Jancu, and C. Katan, J. Phys. Chem. Lett. **4**, 2999 (2013).

[81] J. Paier, R. Asahi, A. Nagoya, and G. Kresse, Phys. Rev. B **79**, 115126 (2009).

[82] J. H. Skone, M. Govoni, and G. Galli, Phys. Rev. B **93**, 235106 (2016).